

# Dynamic phase coexistence and non-Gaussian resistance fluctuations in VO<sub>2</sub> near the metal-insulator transition

Sudeshna Samanta\* and A. K. Raychaudhuri†

*Department of Condensed Matter Physics and Materials Science, Unit for Nanoscience,  
S. N. Bose National Centre for Basic Sciences, Kolkata, India*

HPSTAR  
151-2015

Xing Zhong and A. Gupta

*MINT Center, University of Alabama, Tuscaloosa, Alabama 35487, USA*

(Received 28 June 2015; revised manuscript received 7 September 2015; published 13 November 2015)

We have carried out an extensive investigation on the resistance fluctuations (noise) in an epitaxial thin film of VO<sub>2</sub> encompassing the metal-insulator transition (MIT) region to investigate the dynamic phase coexistence of metal and insulating phases. Both flicker noise as well as the Nyquist noise (thermal noise) were measured. The experiments showed that flicker noise, which has a  $1/f$  spectral power dependence, evolves with temperature in the transition region following the evolution of the phase fractions and is governed by activated kinetics. Importantly, closer to the insulating end of the transition, when the metallic phase fraction is low, the magnitude of the noise shows an anomaly and a strong non-Gaussian component of noise develops. In this region, the local electron temperature (as measured through the Nyquist noise thermometry) shows a deviation from the equilibrium bath temperature. It is proposed that this behavior arises due to current crowding where a substantial amount of the current is carried through well separated small metallic islands leading to a dynamic correlated current path redistribution and an enhanced effective local current density. This leads to a non-Gaussian component to the resistance fluctuation and an associated local deviation of the electron temperature from the bath. Our experiment establishes that phase coexistence leads to a strong inhomogeneity in the region of MIT that makes the current transport strongly inhomogeneous and correlated.

DOI: [10.1103/PhysRevB.92.195125](https://doi.org/10.1103/PhysRevB.92.195125)

PACS number(s): 71.30.+h, 72.70.+m, 71.27.+a

## I. INTRODUCTION

The metal-insulator transition (MIT) in vanadium dioxide (VO<sub>2</sub>) has been a topic of considerable interest [1–5]. The MIT occurs on cooling at  $\approx 341$  K [4] and in films the transition leads to a jump in resistivity by about 3–4 orders in a narrow temperature interval. The capability to grow a controlled VO<sub>2</sub> film with well defined oxygen stoichiometry and vanadium valency, the availability of sensitive measurements from a new perspective, as well as progress in understanding the physics of the transition are some of the reasons that led to the revival of the interest on this material in recent times [5]. In addition to basic physics issues the revival of interest is also due to its emerging application potentials in different polymorphs of VO<sub>2</sub>.

The MIT in VO<sub>2</sub> is strongly linked to changes in the crystallographic lattice in addition to the change in the electrical resistivity. VO<sub>2</sub> undergoes a first-order crystallographic phase transition from a high-temperature metallic tetragonal rutile (RU) phase to a low-temperature insulating monoclinic (MO) phase. An anomaly in the elastic modulus and its softening [6], a reduction of the optical transmittance across the visible and infrared regions of the electromagnetic spectrum [7,8], have been observed at MIT. The MIT can be tuned by doping [9] or by elastic strain [10]. Hence the strong coupling of the electronic and structural degrees of freedom makes the MIT in this material complex as well as fascinating. There are recent

reports on decoupling of the structural and electronic phase transitions at fast time scales in VO<sub>2</sub> nanobeams placed on specific substrates [11]. Some results support the opening of the insulating band gap to the Peierls dimerization, while others attributed the effect to the Coulomb repulsion between localized vanadium  $3d$  electrons [12–15]. Hence, the origin of the metal-insulator phase transition in VO<sub>2</sub> still remains an open question.

The existence of a structural phase transition accompanied by an electronic transition in the same temperature range and their coupling makes the MIT VO<sub>2</sub> special and provides features that may not be present in other such temperature driven MIT. As a result, considerable current attention has been given to the phase coexistence in VO<sub>2</sub> around the temperature region of the MIT. The coexistence occurs between the high-temperature metallic (M) phase and the low-temperature insulating (I) phase. On cooling, the metallic phase fraction ( $f_r$ ) continuously decreases from 1 and  $\rightarrow 0$  on completion of the transition. There are suggestions that the coexistence of macroscopically small metal and insulating domains make the transition of a percolative nature [16–18]. The nature of the coexisting phases can be tuned by strain where compressive strain stabilizes the metallic phase and allows it to continue to lower temperatures on cooling.

In this paper, we investigate the important question of phase coexistence in VO<sub>2</sub> near MIT using the sensitive probe of resistance noise spectroscopy. While past experiments have established the phase coexistence in the MIT region, the issue of the dynamic nature of the phase transition has not been addressed before. The resistance noise spectroscopy allows us to explore the dynamic nature of phase coexistence and also the time scale associated with its dynamics. The dynamical

\*Corresponding author: [sudeshna.samanta@hpstar.ac.cn](mailto:sudeshna.samanta@hpstar.ac.cn); present address: Centre for High Pressure Science & Technology Advanced Research, Shanghai, China.

†[arup@bose.res.in](mailto:arup@bose.res.in)

nature is related to the time variation associated with the coexisting phases. Near MIT, the co-existing phases can be static without any dynamic nature associated with them that would allow a transition from one phase to another. In such a static situation, we would not observe any resistance noise. However, if there is a potential barrier that separates them, then by thermal activation it is possible for the co-existing phases to have a dynamic transition from one to the other while maintaining the average concentration unchanged. This dynamic transition will be slow if the barrier separating them is appreciable. Such a dynamic phase co-existence will lead to low-frequency resistance fluctuations as has been observed here. This particular aspect that there can be a low-frequency (long time) dynamic nature associated with the phase coexistence has not been addressed before. In this investigation, we study this particular aspect. We find that the observed resistance fluctuation has a temperature dependence that shows an activated behavior with activation energy. The mean square resistance fluctuation shows a clear dependence on the metallic fraction  $f_r$  as determined from the evolution of the resistivity  $[\rho(T)]$  with temperature ( $T$ ) near the MIT. We observed that the dynamic nature of the coexisting phases gives rise to substantial low-frequency resistance fluctuations (with spectral power density  $\sim 1/f$ ) at the transition region that also reflects the thermal evolution of the coexisting phases and their nanoscale phase separation [19–23]. We also find a strong non-Gaussian component (NGC) of the resistance fluctuation arising from the coexistence phases over a temperature range around MIT. Interestingly, this NGC of the fluctuation peaks around the temperature region where the metallic phase likely exists in a small pocket with the metallic fraction  $f_r < 10^{-2}$ . We suggest that a local decoupling of the electronic temperature (as measured by the Nyquist noise thermometry) from the overall lattice temperature around MIT is likely to occur. This observation being a new component adds a separate dimension to the MIT in this material. The local decoupling of the electron temperature from the lattice temperature may provide the genesis for the electric-field-driven MIT and an avalanche break down in microscale  $\text{VO}_2$  structures reported recently [9,14,15,24]. The noise spectroscopy along with high-precision resistance data provide evidence that there is a likelihood of occurrence of more than two phases, as reported recently in elastic experiments on  $\text{VO}_2$  nanobeams [11].

One important lesson that has been emerged from our investigation is that in the MIT region, when the metallic fraction goes down, the current will have severe crowding in paths that have the pockets of metallic islands. This makes the current distribution extremely inhomogeneous. Analysis of transport data where current flow is assumed uniform will lead to erroneous inferences. Some of these issues addressed to in this paper have not been investigated before.

## II. EXPERIMENTAL

Well characterized epitaxial thin films of  $\text{VO}_2$  used in our work has been grown by low-pressure chemical vapor deposition on crystalline  $\text{TiO}_2(100)$  [25] within the optimized growth window [5,26] in terms of oxygen flow rate, and substrate temperature. The film growth rate monitored was  $(2.5 \pm 0.2)$  nm/min to avoid very rough film surfaces. The surface

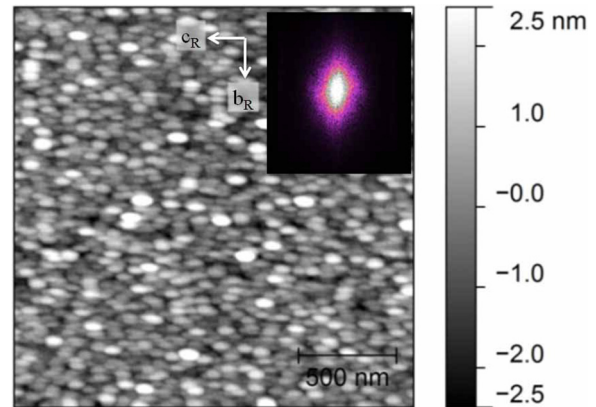


FIG. 1. (Color online) AFM height map of a 35-nm  $\text{VO}_2$  epitaxial thin film grown on a  $\text{TiO}_2$  substrate. The elliptical grains with major axis along parallel to the  $\text{TiO}_2$   $c_R$  axis as seen in the 2D-Fourier transformation image in the inset.  $b$  and  $c$  axis of the substrate are indicated by the arrows.

morphology of the  $\text{VO}_2$  film was studied by atomic force microscopy (AFM) as shown in Fig. 1. The elliptical grains with a major axis along the  $\text{TiO}_2$   $c_R$  axis, seen in the 2D-Fourier transformation image as shown in the inset of Fig. 1. We have used the film of 35 nm with RMS roughness  $\sim 1$  nm. More details on growth and characterization are given elsewhere [25,27].

High-precision resistivity measurements were carried out in four-probe geometry using a phase sensitive detection scheme. The resistance measurements have a resolution about  $\sim \pm 10$  ppm. The resistance noise measurements were done with a low-biasing current  $I = 1 \mu\text{A}$  in five-probe geometry [28] with an ac current detection technique [29]. This allows simultaneous measurement of the Nyquist noise (thermal noise) as well as the flicker noise in excess of the Nyquist noise [30]. The investigation utilizes both the noise data. For electrical measurements including noise measurements Cr/Au (10 nm/100 nm) contact pads have been used. The schematic of the measurement is shown in Fig. 2(a).

The spectral power density (PSD) as well as the probability distribution function (PDF) for the resistance fluctuation were measured by using various digital signal processing schemes from the stored time series of resistance fluctuations [31]. The frequency window of the noise spectrum in our experiment is  $0.1 \text{ Hz} \leq f \leq 10 \text{ Hz}$ . The second spectrum that measures the extent of non-Gaussian noise, was also measured from the time series. Noise measurements can measure a minimum spectral power density of about  $2 \times 10^{-20} \text{ V}^2/\text{Hz}$  that defines the noise floor of our measurement system. Such a low-noise floor also allows us to determine the bias independent Nyquist noise as well as the bias dependent flicker noise (typical  $1/f$  noise). The issue of the Nyquist noise will be taken up later in the discussion section when we discuss the electron temperature. For the rest of the paper, the noise referred to is the flicker noise where the Nyquist noise has been subtracted out.

## III. RESULTS

### A. Resistivity in the transition region

In Fig. 2(b), we show typical resistivity data recorded under thermal cycling. The sample was heated to a higher

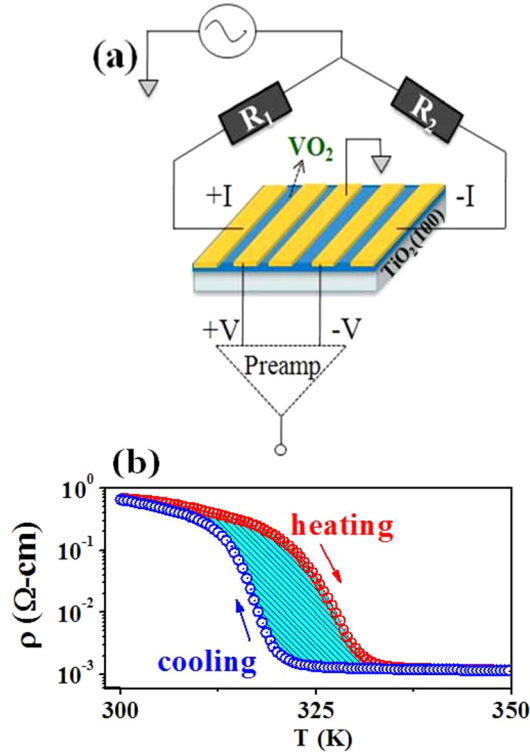


FIG. 2. (Color online) (a) Schematic of the circuit for ac five-probe noise measurements. (b) Resistivity ( $\rho$ ) vs temperature ( $T$ ) plot of the epitaxial thin film of  $\text{VO}_2$  showing the insulator-metal transition for heating and cooling cycles.

temperature ( $\approx 360$  K) where the sample is in the low-resistivity phase. We cooled the sample with a controlled cooling rate 1 K/min to a particular temperature ( $T_{\text{cooled}}$ ) without any biasing current. Starting from that  $T_{\text{cooled}}$ , the  $\rho$ - $T$  data for a heating cycle have been collected on warming with a biasing current  $1 \mu\text{A}$  with a ramp rate 1 K/min. The data in a cooling cycle were acquired in a subsequent cooling cycle. A thermal hysteresis appeared with heating and cooling cycles as plotted in Fig. 2(b) where  $T_{\text{cooled}} = 300$  K. It is noted that the  $\rho(T)$  is dependent on the degree of undercooling (the temperature  $T_{\text{cooled}}$  to which it was cooled before warming). The dependence of  $\rho(T)$  on undercooling likely arises from the differences in phase fractions of the coexisting phases. To ensure that the resistance fluctuation is measured in a sample with a well defined state (i.e., given phase fraction of coexisting phase), we carried out the noise measurements presented below on a sample with  $T_{\text{cooled}} = 300$  K.

From the resistivity shown in Fig. 2(b), we obtain the metallic fraction  $f_r$  using a two-phase model as described previously [25] where the resistivity is given as

$$\rho = \frac{\rho_r \rho_m}{f_r \rho_m + (1 - f_r) \rho_r}, \quad (1)$$

where  $\rho_r$  is the resistivity of the metallic phase,  $\rho_m$  that in the insulating phase.  $f_r$  is the fraction of the metallic phase. The dependence of  $f_r$  on  $T$ , obtained from the Eq. (1), is shown in Fig. 3. It is found that  $T$  dependence of  $f_r$  follows the relation:  $f_r(T) = 1/(1 + A \exp(W_f/k_B T))$ . The value of the activation energy  $W$  is determined to be equal to 3.98 eV. The evolution

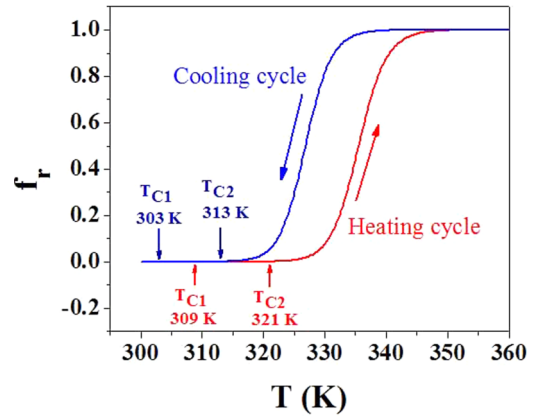


FIG. 3. (Color online) The evolution of the metallic fraction  $f_r$  as a function of  $T$  for heating and cooling cycle. The temperatures marked  $T_{C1}$  and  $T_{C2}$  were obtained from the resistivity derivatives (see Fig. 5).

of the phase fraction as a function of  $T$  in the MIT region is an important parameter and later we show that the evolution of  $f_r$  is closely linked to the evolution of the resistance fluctuations.

## B. Resistance fluctuation

The resistance fluctuation was recorded as a time series of voltage fluctuation  $\Delta V$  from a current biased balanced bridge [see Fig. 2(a)]. To ensure that the sample is in a given thermodynamic state (as there is a hysteresis in the resistivity), the order of thermal cycles is as follows: (a) warming up the sample to 360 K (no bias), (b) from 360 K, cooling down to  $T_{\text{cooled}} = 300$  K (no bias), and then (c) on warming up with current bias to above 360 K (heating cycle) followed by (d) subsequent cooling from 360 to 300 K with the same bias (cooling cycle). At each temperature, the resistance fluctuation  $\Delta\rho(t)$  was collected for 15 min. The total time series data have  $9.2 \times 10^5$  points from which different statistical analyses were made. The fluctuation  $\Delta\rho(t)$  are free from thermal drift as the data are taken by stabilizing the temperature at a given value with accuracy  $\approx 5$  mK. The resistance fluctuation data  $\Delta\rho(t)$  taken with a current bias of  $I = 1 \mu\text{A}$  are shown in Fig. 4(a) for five representative temperatures in the transition range covering a temperature range 300 to 350 K. There is a steady increase in the fluctuation in resistivity as the sample is cooled through the transition region. The resistivity fluctuation in the insulating region ( $T \approx 315$  K) is about 100 times more than that in the metallic region ( $T \approx 350$  K). In the metallic phase, the resistance fluctuation is expected to arise only from fluctuations in mobility. In the insulating phase, the carrier concentration goes down by several orders and the carrier density fluctuation adds a significant component in enhanced fluctuation.

The normalized power spectral density (PSD) of resistance fluctuation (flicker noise) for few representative temperatures at heating and cooling thermal cycles are shown in Fig. 4(b). The PSD of the noise  $S_\rho(f)/\rho^2 \propto 1/f^\alpha$  with  $\alpha \approx 1.1$ . PSD at different  $T$ , retains its  $1/f$  spectral signature. The PSD increases with increasing  $T$ . This is because the PSD is normalized by the resistivity  $\rho(T)$  at that temperature. Since in

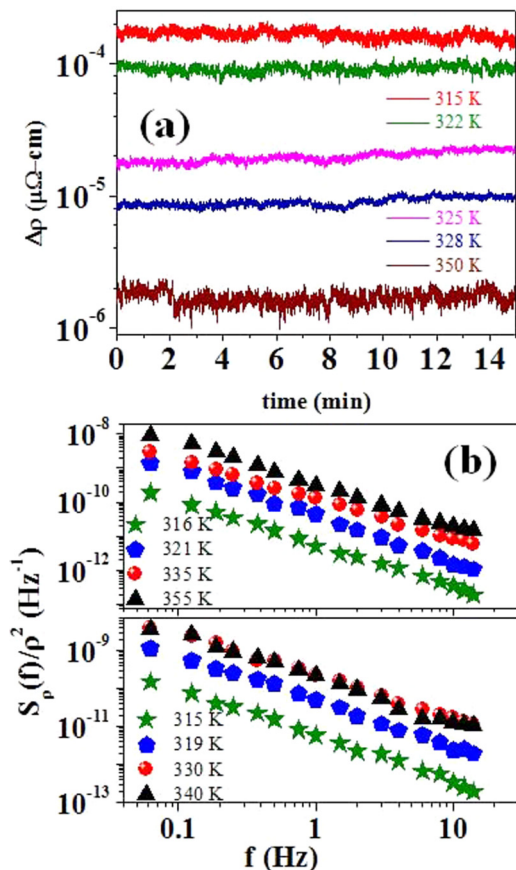


FIG. 4. (Color online) (a) Time series of resistivity fluctuations  $\Delta\rho(t)$  at five different representative temperatures encompassing insulator-metal transition. (b) Power spectral density (PSD)  $S_\rho(f)/\rho^2$  at different temperatures for the same thermal cycles. The PSD shows  $1/f$  spectral dependence.

the high- $T$  phase  $\rho(T)$  has a very low value compared to that in the low- $T$  phase, the normalized PSD increases on heating as the  $\rho^2(T)$  is in the denominator.

The temperature variation of the mean square fluctuation (MSF), the variance  $\langle(\Delta\rho)^2\rangle$  is shown in Fig. 5 for both heating and cooling cycles. The MSF was calculated by integrating the spectral power density PSD over the frequency range of our experiment ( $0.1 \text{ Hz} \leq f \leq 10 \text{ Hz}$ ), i.e.,  $\langle(\Delta\rho)^2\rangle = \int_{0.1\text{Hz}}^{10\text{Hz}} S_\rho(f)df$ . The MSF changes by four orders in a narrow temperature range. The  $T$  dependence of MSF closely resembles the  $\rho$  versus  $T$  data, including the hysteresis. The  $T$  variation of the MSF saturates when the  $T$  dependence of  $\rho(T)$  also saturates at both ends of the transition region. This can be nicely seen when we compare the  $T$  dependence of MSF with the resistance derivative  $d\rho/dT$  shown in Fig. 5. It can be noted that while for most of the MIT region the fluctuation evolves following the evolution of  $\rho(T)$ , there is a narrow temperature region where there is clear departure from the smooth evolution. The anomalous features are marked by arrows and referred to as temperatures  $T_{C1}$  and  $T_{C2}$  where the temperature derivatives of  $\rho$  show extrema (see Fig. 5). The feature is clearer in the heating curve and there is almost an order of magnitude change over a temperature interval of a few degrees of Kelvin. These features are reproducible.

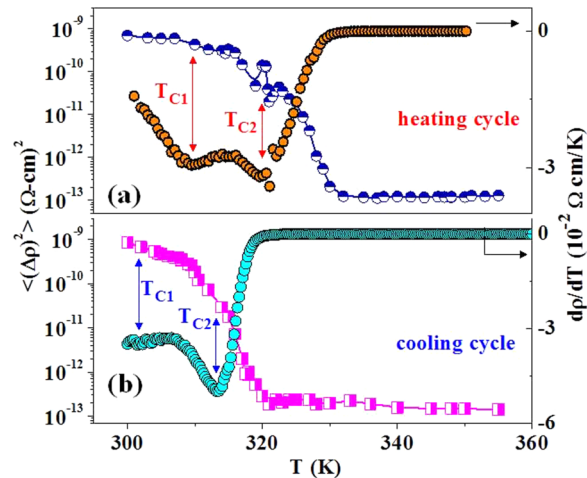


FIG. 5. (Color online) Mean-square resistivity fluctuations  $\langle(\Delta\rho)^2\rangle$  along with the derivative of resistivity  $d\rho/dT$  plotted as a function of  $T$  for both heating and cooling cycles.

### C. Resistance fluctuation and phase-coexistence

The resistance fluctuation was found to change with temperature as the MIT region is traversed. We show below that the noise has a close link with the evolution of the phase fractions as quantified through  $f_r$ . This indeed is a very important result because it directly relates the fluctuation to coexistence of phases. We show a plot of the normalized variance  $\langle(\Delta\rho)^2\rangle/\rho^2$  with the metallic fraction  $f_r$  in Fig. 6. The normalized variance evolves monotonically with the metallic fraction  $f_r$  for most of the region. The data for  $f_r$  are shown in a logarithmic plot to accentuate the low- $f_r$  region where we see interesting features. The heating and cooling curves mostly follow each other barring the region  $f_r \sim 0.1$ . The heating and cooling processes may change the exact fraction of the two coexisting phases leading to the difference in the variance for heating and cooling curves.

Interesting features are seen in the region around  $T_{C1}$  and  $T_{C2}$  where one observes anomalous features where the dependence of  $\langle(\Delta\rho)^2\rangle/\rho^2$  on  $f_r$  deviates from the monotonous

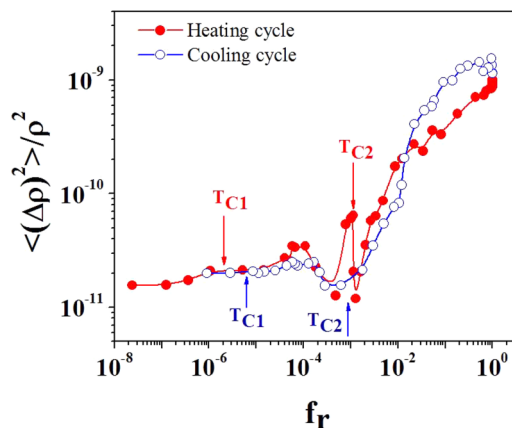


FIG. 6. (Color online) Normalized MSF  $\langle(\Delta\rho)^2\rangle/\rho^2$  as a function of metallic fraction  $f_r$  for two thermal cycles showing anomalies near  $T_{C1}$  and  $T_{C2}$ .

behavior. The deviation is more visible in the heating cycle. The asymmetry of the heating and cooling cycle will be discussed later on in the discussion section. Importantly, these features occur in the region where the metallic fraction is rather low and typically  $f_r \leq 10^{-3}$ . However, due to the much larger conductivity of the metallic phase, the fraction of current going through the metallic region is rather high ( $\approx 0.3-0.5$ ). This would imply that a large current will preferentially flow through paths that contain small but finite pockets of metallic islands. This will make the current path inhomogeneous leading to an enhanced current density in certain regions of the sample. We show below that in this temperature region, large non-Gaussian fluctuations show up. The issue of the existence of small metallic pockets in the insulating phase has been suggested from ac conductivity measurements [32]. The noise experiments confirm their existence.

**D. Activated dynamics of resistance fluctuation**

The experimental results in previous subsections clearly show that the resistance fluctuation has a clear link to the phase coexistence. Resistance fluctuations also carry information about the frequency and time scale associated with it. The dynamic technique as a noise measurement clearly establishes that the coexisting phases are not static but dynamic in nature. The kinetics of the coexisting phases manifests PSD of  $1/f$  nature, which suggests that the frequency/time scale associated with the fluctuation may have a much broader spectral range.

The observed fluctuation has a substantial low-frequency (long-time-scale) component that generally can arise if the coexisting phases contributing to the fluctuation have a dynamic equilibrium that is thermally activated. To check this hypothesis, we calculated the parameter  $K = S_\rho(f = 1 \text{ Hz})\Omega/\rho$  ( $\text{cm}^2/\text{ohm}$ ), which is often used to compare the noise between different solids [33].  $\Omega$  is the volume of the solid used for noise measurements. The value of  $K$  as a function of temperature (plotted against  $1/T$ ) is shown in Fig. 7. We find that  $K$  follows an activated temperature dependence (marked by a line) with activation energy  $W_n \approx 4.04 \text{ eV}$ . This activation energy is the energy barrier for conversion between the two coexisting phases. Importantly, this matches

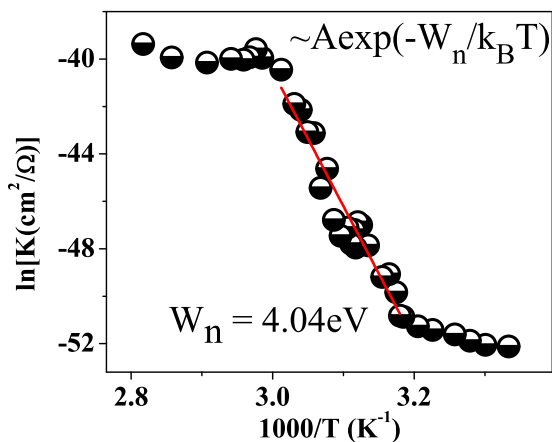


FIG. 7. (Color online) Noise parameter  $K$  as a function of reciprocal temperature. The  $T$  dependence of  $K$  gives an activation energy  $W_n = 4.04 \text{ eV}$ .

very closely with the value of  $W_f$  obtained independently from the temperature dependence of the metallic fraction  $f_r$ , as done in a previous subsection. The close match of the two activation energies thus relates the dynamics of resistance fluctuation to the coexisting phases and also establishes that the nature of dynamic equilibrium is through an activation barrier.

**E. Non-Gaussian nature of resistance fluctuation**

It is observed that in the temperature window  $T_{C1} < T < T_{C2}$  where the fluctuation shows anomalous behavior, the resistivity fluctuation becomes non-Gaussian. The existence of a non-Gaussian component (NGC) to the fluctuation has been established by two tools discussed below.

A direct way to establish NGC is to look at the Probability distribution function (PDF) of the fluctuation. For a Gaussian fluctuation (which we record as time series of voltage fluctuation  $\Delta V$ ), the probability distribution  $[P(\Delta V)]$  is given as

$$P(\Delta V, \mu, \sigma) = \frac{1}{\sigma\sqrt{2\pi}} \exp\left[-\frac{(\Delta V - \mu)^2}{2\sigma^2}\right], \quad (2)$$

where  $\mu$  is the mean and  $\sigma$  is the standard deviation of the distribution. For a Gaussian distribution of PDF, the magnitude of fluctuation should be such that a plot of  $\ln P(\Delta V)$  versus  $(\Delta V)^2$  should be linear. Any deviation from the linearity will signify presence of a non-Gaussian component of the resistance fluctuations. In Fig. 8, we show a plot of  $\ln P(\Delta V)$  versus  $(\Delta V)^2$  at three representative temperatures both for heating and cooling cycles. One temperature is close to where we see the anomalous noise ( $T \approx T_{C1}$  or  $T \approx T_{C2}$ ) and two temperatures are few Kelvins above and below. It can be clearly seen that while for  $T$  above and below the characteristic temperature region the  $\ln P(\Delta V)$  versus  $(\Delta V)^2$  is a straight line over an extensive range of the fluctuation, at the

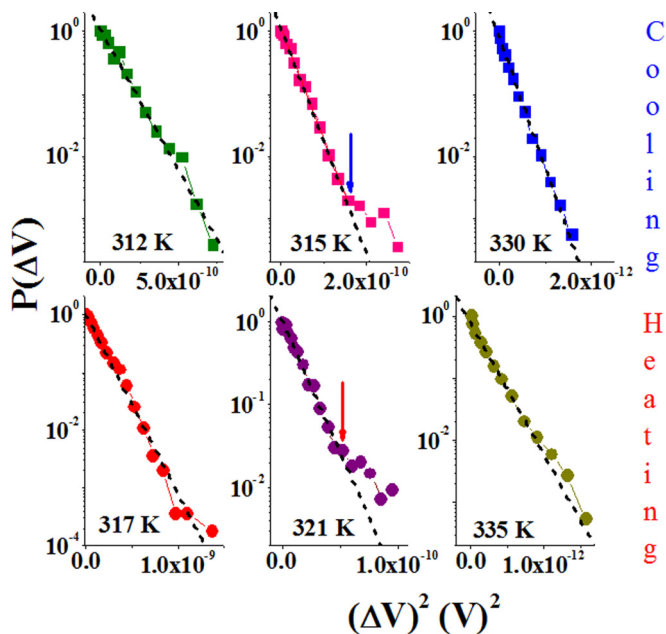


FIG. 8. (Color online) Temperature evolution of  $\ln P(\Delta V)$  vs  $(\Delta V)^2$  near MIT. The arrows show deviation from Gaussian behavior.

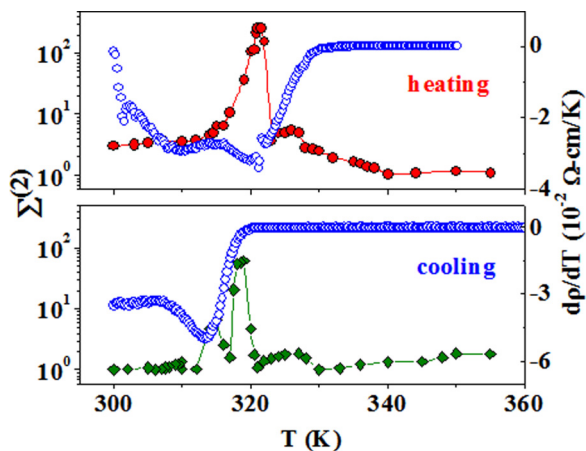


FIG. 9. (Color online) Variation of the normalized variance of integrated second spectra with  $T$  for heating and cooling cycles.  $\Sigma^{(2)}$  is maximum in phase transition region.

characteristic temperatures there are significant deviation from the straight line (marked by arrow in Fig. 8). The deviation implies that there are occasional large fluctuations that do not follow Gaussian distribution.

Another useful tool to diagnose existence of NGC in the fluctuation is to evaluate the higher order statistics of the fluctuation. Higher-order statistics [29,34] like the second spectrum can be used to quantify the NGC of noise. The second spectrum (SS)  $s^2(f_2)$  is defined as

$$s^2(f_2) = \frac{\int_0^\infty \langle \Delta\rho^{(2)}(t)\Delta\rho^{(2)}(t+\tau) \rangle \cos(2\pi f_2\tau) d\tau}{\left[ \int_{f_L}^{f_H} S_\rho(f_1) df_1 \right]^2}, \quad (3)$$

where  $f_1$  and  $f_2$  are the frequencies associated with first and second spectrum respectively. The second spectrum has been calculated within the frequency band 2 Hz [ $f_H(3$  Hz)– $f_L(1$  Hz)], where  $f_1 = 2$  Hz.

The temperature dependence of  $s^2(f_2)$  shows how the correlated fluctuation builds up in the temperature region of the MIT. In Fig. 9, the temperature evolution of the integrated second spectra  $\Sigma^{(2)}$  are shown for both heating and cooling cycles.  $\Sigma^{(2)} = \int_0^{f_H-f_L} s^2(f_2) df_2$ , which is the second spectrum  $s^2(f_2)$  integrated within the experimental bandwidth. Figure 9 shows very clearly that in the temperature range where the phase-coexistence contributes to variance, the NGC also becomes high. In the same graph, we also plotted the resistivity derivative curves. At  $T < T_{C2}$ ,  $\Sigma^{(2)}$  rises sharply and it is maximum at  $T = T_{C2}$ . Again,  $\Sigma^{(2)}$  drops sharply just above  $T_{C2}$ . Repeated measurements confirm the reproducibility of this sharp feature in  $\Sigma^{(2)}$ . The NGC is absent when the phase is either almost pure metallic RU ( $f_r \approx 1$ ) at high-temperature end or almost insulating MO ( $f_r \approx 0$ ) at low-temperature end. NGC is finite in the range when both phases are coexisting, in particular in the range where the metallic fraction exists in small pockets. The sharp change of  $\Sigma^{(2)}$  as a function of temperature in certain range, is a manifestation of the coexisting phases with widely differing conductivities and the percolative nature of the current transport.

## IV. DISCUSSION

The results presented above show that there is a rich behavior of the resistance fluctuation as the material is heated and cooled through the transition region. The fluctuation evolves as a function of  $T$  as the MIT region is traversed. There are a number of features in the noise data that would need discussion as they point to some new features/new information on the MIT that have not been observed before through measurements of resistivity alone. They also point to the a rather complex nature of the MIT in  $\text{VO}_2$ . In the following part, some of the important observations are discussed to highlight their significance in the general context of the temperature driven MIT in  $\text{VO}_2$ . Some of the features may even be general enough that they can be observed in other temperature driven MIT like that in the rare-earth nickelates.

### A. The fluctuators

In general, in metals with fixed carrier density  $n$ , the fluctuation originates from mobility fluctuations where there is a dynamics in the scattering cross-section that shows up in the frequency dependence of the PSD. In insulators, the resistance fluctuation mainly comes from carrier density fluctuations that take the form of generation-recombination (GR) noise as in conventional doped semiconductors [30]. The Hall effect [35] measurements in  $\text{VO}_2$  thin films across the metal-insulator transition show that the hall carrier density ( $n$ ) changes by several orders of magnitude at the transition from  $4 \times 10^{18} \text{ cm}^{-3}$  (in insulating MO phase) to  $1.4 \times 10^{23} \text{ cm}^{-3}$  (in metallic RU phase). However, the Hall carrier mobility changes nominally over the same temperature range. The MIT is thus accompanied by substantial carrier depletion (release) on cooling (heating) as one goes through the transition. The large change in  $n$ , that accompanies the MIT is the cause of the evolution of the magnitude of the noise across the temperature. The role of existence of inhomogeneous current path also enhances the magnitude of the noise and as we will discuss below, can lead to strong non-Gaussian transition. A strong built up of very large noise in systems with few carriers are also seen in the vicinity of disorder driven Anderson type MI transition seen in doped semiconductor like P doped Si with carrier concentration  $n \approx n_c$ , where  $n_c$  is the critical concentration of the MI transition [36].

### B. Anomalous noise behavior and NGC

The anomalous noise behavior as well as NGC in the temperature range around  $T_{C2} < T < T_{C1}$  occur when the metallic fraction  $f_r$  is very low (see Fig. 6). At this small metallic fraction, one does not expect a percolative metallic path extending over the whole sample volume. The small value of  $f_r$  would suggest existence of isolated metallic pockets that occur within a majority insulating phase. It has been suggested that in the majority insulating phase the conduction is by polarons tunneling between isolated metallic islands [27]. In such a case, one would have charging and discharging of the metallic islands. This phenomena can give rise to large noise although there may be few such metallic islands in the regime of low  $f_r$ . The relatively long time associated with such

a charging-discharging of metallic islands through insulating paths will contribute to low-frequency fluctuations.

It is suggested that the finite NGC arise from the transport through a system that has such sparse distribution of metallic islands. This makes the current path develop a correlation by a random (and dynamic) time-dependent distribution of current paths [37]. Such a re-distribution leading to substantial NGC arises over a narrow temperature window. For higher metallic fraction, the currents go through regions that are predominantly metallic without the need for dynamic current redistribution. At much lower  $f_r$ , the fraction of the current carried by the metallic phase fraction (ratio) is very small, hence its contribution to the observed fluctuation is not perceptible and the time scale associated may be much longer than the lowest-frequency limit of the measurements.

### C. Does the electron loose equilibrium with the lattice in the transition region?

The phase coexistence that occurs in the region of MIT is expected to be in thermal equilibrium even though the coexisting phases have a temperature driven transition from one phase to another maintaining a dynamic equilibrium. It is expected that since the time scale associated with the dynamic phase coexistence is long, the electronic system will maintain thermal equilibrium with the lattice. Though it is an expectation, it has never been tested experimentally. Noise measurement, particularly measurement of the Nyquist noise offers a direct way to check this. The Nyquist noise is the thermal noise of a resistor of value  $R$  connected to a thermal bath kept at temperature  $T$ . The white SPD is given as  $S_{th} = 4k_B T R$ ,  $k_B$  being the Boltzman constant [38]. The Nyquist noise offers a direct way to measure the temperature electronic system  $T_e$  [39]. For an electronic system in equilibrium with the thermal bath provided by the lattice  $T_e \approx T$ , where  $T$  is the equilibrium lattice temperature. If  $T_e \neq T$ , this would imply that the electron bath has lost the thermal equilibrium with the phonon heat bath locally.

In case of a phase transition in  $\text{VO}_2$  where in a certain temperature range there is current crowding and transport through sparse metallic islands, it is not unlikely that the current density deviates strongly from what is expected from uniform current distribution. Such inhomogeneous current distribution will not only lead to NGC, as discussed before, but can actually give rise to nanoscopic hot regions where the temperature can differ from the average lattice temperature. This will lead to local hot electrons that have  $T_e > T$ . Such a local heating has been seen in ferromagnetic insulating phases of manganites [40]. In Fig. 10, we plot the measured  $T_e$  obtained from the Nyquist noise as a function of the lattice temperature. The dotted line shows the equilibrium line where  $T_e = T$ . It is very interesting to see that the equilibrium of the electron system is maintained at all temperatures in the MIT interval except the region around  $T_{c1} < T < T_{c2}$ . In this region,  $T_e > T$ , the deviation is noticeable particularly in the heating cycle. This is the specific temperature range where we find the noise is anomalous and also shows substantial NGC. It is to be noted that such a deviation of separation of  $T_e$  and  $T$  has not been observed before in such phase transitions. It clearly brings out that the nonlinear current distribution at

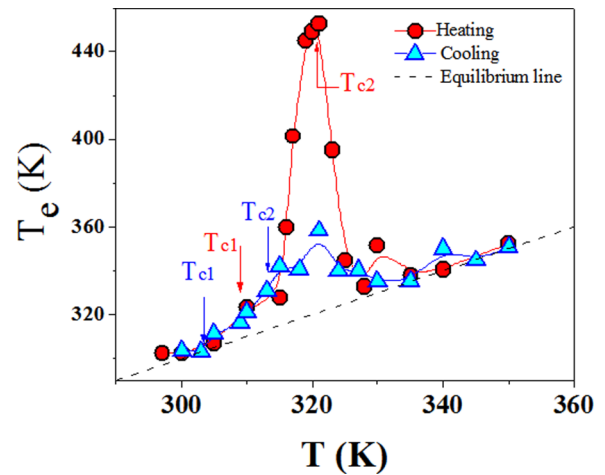


FIG. 10. (Color online) The electronic temperature ( $T_e$ ) as obtained from Nyquist noise, as a function of phonon bath temperature  $T$ .

some regions can lead to current crowding that can lead to such a nonequilibrium situation. The magnitude of the local deviation of the electron temperature will depend on thermal quantities like the specific heat of the coexisting phases as well as the thermal conductivity that can ensure efficient heat transfer from the regions of high current density. In recent years, there are reports of voltage driven MIT in  $\text{VO}_2$  films as well as avalanche-type breakdown [24]. We propose that the origin of such phenomena can lie at the local departure of the electron temperature from the equilibrium lattice bath as has been directly observed by Nyquist noise thermometry.

### D. Asymmetry in heating and cooling curves

In general, thermal cycling in a first-order phase transition gives rise to a hysteresis showing differences in heating and cooling curves. It is observed that the anomalies in the noise data, NGC, and the deviation of  $T_e$  from the thermal equilibrium values are more prominent in the heating cycle than that seen in the cooling cycle. These differences between the two cycles (asymmetry) may be small but they are clearly discernible. It is suggested that this may have a thermodynamic/kinetic origin as that occurs in supercooled systems loosing thermal equilibrium. While cooling down from the high-temperature phase, the equilibrium phase is the conductive RU phase. The history of the past thermal cyclings is annealed out and there is no frozen low-temperature MO phase. The low-temperature phase sets in on cooling and coexists with the high-temperature phase, which eventually becomes a minority phase ( $f_r \rightarrow 0$ ) on further cooling. It can happen that in the cooling cycle the high- $T$  phase fraction does not become completely zero but a small fraction remains frozen in due to kinetic reasons. The frozen in phase part is in excess of the thermal equilibrium value. On heating, these small metallic pockets acquire more thermal energy and tend to reach thermal equilibrium leading to the observed anomalies as well as the current redistribution that gives rise to the signature of the NGC. It is therefore suggested that the asymmetry in the heating and cooling curves has a thermodynamic/kinetic

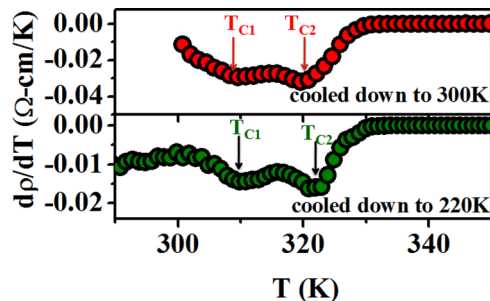


FIG. 11. (Color online)  $d\rho/dT$  vs  $T$  plot for two representative undercooling temperatures  $T_{\text{cooled}}$  showing the evolution of transition doublets when the sample is cooled down to 300 and 220 K.

origin that determines the nature of phase equilibrium of the two phases.

### E. Possibility of more phases coexisting in the MIT region

The existence of the doublet in the resistivity derivatives (see Fig. 5) at temperatures  $T_{C1}$  and  $T_{C2}$  and raises the possibility of more than two coexisting phases in the MIT region. In general, a smooth resistivity curve like that shown in Fig. 2(b) should show one derivative maximum where  $\rho$  changes most with  $T$ . We find that there is consistent existence of two resistivity derivative maxima, which we refer to as the derivative doublet. The position of the doublet changes also on heating and cooling cycles. To check that there is indeed a connection of the derivative doublet to coexisting phases we measured the resistivity in heating cycles after cooling to different temperatures. In Fig. 11, we show the derivative doublets at two values of  $T_{\text{cooled}} = 300$  and 220 K. It can be seen that it leads to an evolution of the derivative doublets. Based on this, we suggest that there may be more than two coexisting phases in the transition region. Such a possibility has been observed in recent nanobeam experiments [16] as well as in structural studies by micro x-ray diffraction ( $\mu$ XRD). It has been observed that there exist more than one low-temperature crystallographic structures, namely, the low-stress monoclinic  $M_1$  and high-stress monoclinic  $M_2$ . The experiments suggest that a pure  $M_1$  structure can be observed between room temperature and a certain temperature band. Moreover, the  $M_2$  and RU structures appear in two different parts within a separate temperature band. A single RU phase was observed throughout the nanobeam for temperatures higher than these two temperature bands. They suggest that the  $M_2$  phase possesses an intermediate crystal structure between  $M_1$  and RU, which allows competition among the free energies associated with them and the regions near the phase transitions appeared to be spatially inhomogeneous. The possible transitions from  $M_1$ -RU and  $M_2$ -RU encompassing MIT can have a strong correlation with the appearance of resistivity doublets. The complex dependence of stress and temperature leads to a percolative nature of the phase transition with the coexistence of macroscopically small metal and insulating domains. It is also suggested that the undercooling changes the phase fraction of these  $M_1$  and  $M_2$  phases and thus

induces a small shift in the derivative doublets. At this stage, it is a suggestion and further investigations will be needed to cleanly settle this issue.

We note that the exact details of the nature of the phase coexistence and the resulting dynamics that are investigated in this paper will depend on the physical form of the sample that will determine the nature of the percolating current paths. For example, the quantitative details of the coexisting phases in a film (as used here) will be different from the details of those coexisting in nanobeams [16]. As a result, some of the specific features of the dynamic phase coexistence as observed in the noise spectroscopy might not be observed, if such experiments are carried on in a nanobeam.

## V. CONCLUSION

We have carried out an extensive investigation of resistance fluctuations (noise) in  $\text{VO}_2$  thin films encompassing the MIT region. The transition shows a large change in resistivity over a small temperature range and is associated with a structural phase transition. The experiment was done primarily to use the measurement of resistance noise as a probe to investigate the dynamic phase coexistence in the transition region. The experiment showed that resistivity fluctuation (flicker noise) arises from dynamic equilibrium of coexisting insulating and metallic phases. The temperature dependence of the fluctuation has a clear dependence on the evolution of the phase fractions as the sample is heated or cooled through the transition region. The dynamic phase-coexistence gives rise to low-frequency fluctuations in the resistance which is governed by activated kinetics that controls the evolution of the phases in the coexistence region as the temperature is changed. The spectral power density has a  $1/f$  dependence over the whole temperature region.

Importantly, closer to the insulating end of the transition, when the metallic phase fraction is low ( $f_r < 10^{-3}$ ), the magnitude of the noise shows an anomaly where the noise also becomes strongly non-Gaussian. The measurement of the electron temperature as done through Nyquist noise thermometry shows that in this region the local electron temperature also deviates from the equilibrium bath temperature.

It is proposed that this non-Gaussian noise, as well as the local rise of the electron temperature over the bath temperature, arise because substantial part of the current (30%–50%) is carried through small metallic islands that are well separated by an insulating matrix. The noise is enhanced in the region due to charging and discharging of these metal islands. In such a situation, current crowding occurs and there is a dynamic redistribution of current paths through these metallic islands. The current distribution becomes correlated giving rise to a non-Gaussian component to the resistance fluctuation. The current crowding through small metallic islands also enhances the local current density that leads to a local deviation of electron temperature from the bath. The experiment clearly shows that in such MIT, the current transport is strongly inhomogeneous and attaches importance to the residual metallic islands in the insulating phase as controlling elements in the current transport.

## ACKNOWLEDGMENTS

The authors at SNBNCBS acknowledge financial support from the Department of Science and Technology, Government of India as a sponsored project (Unit for Nanoscience). A.K.R.

thanks J.C. Bose Fellowship (SERB) for additional financial support. The work at the University of Alabama was supported by the National Science Foundation under Grant No. DMR-0706280.

- 
- [1] F. J. Morin, *Phys. Rev. Lett.* **3**, 34 (1959).
- [2] I. G. Austin and N. F. Mott, *Science* **168**, 71 (1970).
- [3] J. B. Goodenough, *Annu. Rev. Mater. Sci.* **1**, 101 (1971).
- [4] M. Imada, A. Fujimori, and Y. Tokura, *Rev. Mod. Phys.* **70**, 1039 (1998); Y. Tokura, *Phys. Today* **56**, 50 (2003).
- [5] Z. Yang, C. Ko, and S. Ramanathan, *Annu. Rev. Mater. Res.* **41**, 337 (2011).
- [6] Nelson Sepúlveda, Armando Rúa, Rafmag Cabrera, and Félix Fernández, *Appl. Phys. Lett.* **92**, 191913 (2008).
- [7] D. Z. Ruzmetov, K. T. Zawilski, V. Narayanamurti, and S. Ramanathan, *J. Appl. Phys.* **102**, 113715 (2007).
- [8] R. Lopez, T. E. Haynes, L. A. Boatner, L. C. Feldman, and R. F. Haglund, *Phys. Rev. B* **65**, 224113 (2002).
- [9] M. Marezio, D. B. McWhan, J. P. Remeika, and P. D. Dernier, *Phys. Rev. B* **5**, 2541 (1972).
- [10] J. M. Atkin, S. Berweger, E. K. Chavez, M. B. Raschke, J. Cao, W. Fan, and J. Wu, *Phys. Rev. B* **85**, 020101 (2012).
- [11] Z. Tao, Tzong-Ru T. Han, S. D. Mahanti, P. M. Duxbury, F. Yuan, C.-Y. Ruan, K. Wang, and J. Wu, *Phys. Rev. Lett.* **109**, 166406 (2012).
- [12] J. I. Sohn, H. J. Joo, D. Ahn, H. H. Lee, A. E. Porter, K. Kim, D. J. Kang, and M. E. Welland, *Nano Lett.* **9**, 3392 (2009).
- [13] A. Cavalleri, T. Dekorsy, H. H. W. Chong, J. C. Kieffer, and R. W. Schoenlein, *Phys. Rev. B* **70**, 161102 (2004).
- [14] M. M. Qazilbash, M. Brehm, B. G. Chae, P. C. Ho, G. O. Andreev, B. J. Kim, S. J. Yun, A. V. Balatsky, M. B. Maple, F. Keilmann, H. T. Kim, and D. N. Basov, *Science* **318**, 1750 (2007).
- [15] B.-J. Kim, Y.-W. Lee, S. Choi, J.-W. Lim, S. J. Yun, H.-T. Kim, T.-J. Shin, and H.-S. Yun, *Phys. Rev. B* **77**, 235401 (2008).
- [16] J. Cao, Y. Gu, W. Fan, L. Q. Chen, D. F. Ogletree, K. Chen, N. Tamura, M. Kunz, C. Barrett, J. Seidel, and J. Wu, *Nano Lett.* **10**, 2667 (2010).
- [17] J. Wei, Z. Wang, W. Chen, and D. H. Cobden, *Nat. Nanotechnol.* **4**, 420 (2009).
- [18] S. Zhang, J. Y. Chou, and L. J. Lauhon, *Nano Lett.* **9**, 4527 (2009).
- [19] A. Frenzel, M. M. Qazilbash, M. Brehm, B.-G. Chae, B.-J. Kim, H.-T. Kim, A. V. Balatsky, F. Keilmann, and D. N. Basov, *Phys. Rev. B* **80**, 115115 (2009).
- [20] Y. J. Chang, J. S. Yang, Y. S. Kim, D. H. Kim, T. W. Noh, D.-W. Kim, E. Oh, B. Kahng, and J. S. Chung, *Phys. Rev. B* **76**, 075118 (2007).
- [21] A. C. Jones, S. Berweger, J. Wei, D. Cobden, and M. B. Raschke, *Nano Lett.* **10**, 1574 (2010).
- [22] J. Kim, C. Ko, A. Frenzel, S. Ramanathan, and J. E. Hoffman, *Appl. Phys. Lett.* **96**, 213106 (2010).
- [23] M. M. Qazilbash, A. Tripathi, A. A. Schafgans, B.-J. Kim, H.-T. Kim, Z. Cai, M. V. Holt, J. M. Maser, F. Keilmann, O. G. Shpyrko *et al.*, *Phys. Rev. B* **83**, 165108 (2011).
- [24] K. Kawatani, H. Takami, T. Kanki, and H. Tanaka, *Appl. Phys. Lett.* **100**, 173112 (2012).
- [25] Xing Zhong, Xueyu Zhang, Arunava Gupta, and P. LeClair, *J. Appl. Phys.* **110**, 084516 (2011).
- [26] Y. Muraoka, Y. Ueda, and Z. Hiroi, *J. Phys. Chem. Solids* **63**, 965 (2002).
- [27] Xing Zhong, P. LeClair, Sanjoy K. Sarker, and Arunava Gupta, *Phys. Rev. B* **86**, 094114 (2012).
- [28] J. H. Scofield, *Rev. Sci. Instrum.* **58**, 985 (1987).
- [29] S. Samanta, A. K. Raychaudhuri, and Ya. M. Mukhovskii, *Phys. Rev. B* **85**, 045127 (2012).
- [30] A. K. Raychaudhuri, *Curr. Opin. Solid State Mater. Sci.* **6**, 67 (2002).
- [31] A. Ghosh, S. Kar, A. Bid, and A. K. Raychaudhuri, [arXiv:cond-mat/0402130v1](https://arxiv.org/abs/cond-mat/0402130v1).
- [32] A.-M. S. Tremblay, S. Feng, and P. Breton, *Phys. Rev. B* **33**, 2077 (1986); A. G. Hunt, *Philos. Mag. B* **81**, 875 (2001).
- [33] L. K. J. Vandamme, *Fluct. Noise Lett.* **10**, 467 (2011).
- [34] G. T. Seidler and S. A. Solin, *Phys. Rev. B* **53**, 9753 (1996); G. T. Seidler, S. A. Solin, and A. C. Marley, *Phys. Rev. Lett.* **76**, 3049 (1996).
- [35] D. Ruzmetov, D. Heiman, B. B. Claffin, V. Narayanamurti, and S. Ramanathan, *Phys. Rev. B* **79**, 153107 (2009).
- [36] S. Kar, A. K. Raychaudhuri, A. Ghosh, H. v. Löhneysen, and G. Weiss, *Phys. Rev. Lett.* **91**, 216603 (2003).
- [37] L. M. Lust and J. Kakalios, *Phys. Rev. Lett.* **75**, 2192 (1995).
- [38] F. Reif, *Fundamentals of Statistical and Thermal Physics* (Waveland Press Inc., Illinois, 2008).
- [39] L. F. Cugliandolo, J. Kurchan, and L. Peliti, *Phys. Rev. E* **55**, 3898 (1997); M. Max, *Phys. Rev.* **109**, 1921 (1958); F. Green, *Phys. Rev. B* **54**, 4394 (1996).
- [40] H. Jain and A. K. Raychaudhuri, *Appl. Phys. Lett.* **93**, 182110 (2008).